

Citation for published version:

Reynolds, T, Chang, W-S & Harris, R 2013, 'In-service dynamic stiffness of dowel-type connections', Paper presented at 46th Meeting of CIB W18 on Timber Structures, Vancouver, Canada, 19/08/13 - 24/10/13.

Publication date:
2013

Document Version
Peer reviewed version

[Link to publication](#)

University of Bath

Alternative formats

If you require this document in an alternative format, please contact:
openaccess@bath.ac.uk

General rights

Copyright and moral rights for the publications made accessible in the public portal are retained by the authors and/or other copyright owners and it is a condition of accessing publications that users recognise and abide by the legal requirements associated with these rights.

Take down policy

If you believe that this document breaches copyright please contact us providing details, and we will remove access to the work immediately and investigate your claim.

In-service dynamic stiffness of dowel-type connections

Thomas Reynolds

Richard Harris

Wen-Shao Chang

BRE Centre for Innovative Construction Materials, Department of Architecture and Civil Engineering, University of Bath, UK

1 Introduction

Checks in Serviceability Limit State are very significant in timber design - probably more so than for other materials. As taller buildings and longer spans are used, the ability to check for dynamic response becomes more important. This paper addresses the need for a simple expression to be derived, for inclusion in Eurocode 5 [1], to model dynamic stiffness of connections.

The effect of connection stiffness on the behaviour of frame structures is modelled by assuming semi-rigid connection behaviour. Eurocode 5 provides rules for calculating the slip modulus, which can be used to assess this connection stiffness for static load. The semi-rigid connection stiffness required for modelling and predicting the in-service dynamic behaviour of dowel-type connections is different to the stiffness appropriate to static loading.

Timber structures in service can be caused to vibrate by the dynamic loads imposed by, for example, footfall, turbulent wind load or vibrating machinery. In the majority of cases, these in-service loads impose one-sided vibration on connections. That is to say, the force in the connection oscillates without reversing, having a non-zero mean. Footfall, for example, imposes a small-amplitude dynamic load in comparison with the mean load applied by the self-weight and imposed loads on the structure. Similarly, the steady component of wind load applies a mean force, around which the turbulent component oscillates.

A process for prediction of the stiffness of connections in these conditions is required to allow effective design of timber structures to meet vibration serviceability criteria. A method is presented here which uses the experimental observation that this form of one-sided vibration exhibits a secant stiffness close to that predicted by elastic analysis of the dowel-timber interaction.

1.1 Current Guidance in Design Codes

Eurocode 5 [1] provides guidance for assessing the stiffness of a single-dowel connection with the implication that the guidance can be extended to allow for an arbitrary number of dowels and shear planes. Separate design guides [2] provide methods for the single-dowel stiffness calculated according to Eurocode 5 to be used to calculate the rotational stiffness of a moment connection. The stiffness K_{ser} given in Eurocode 5 allows for deformation of

timber and connector in one empirical expression, and is independent of the geometry of the connection, relying only on the diameter of the connector and the density of the timber.

This literature review has not found details of the empirical derivation of the current Eurocode model for connection stiffness. The only reference which has been found is Ehlbeck and Larsen's statement [3] that it was derived by regression analysis of a large number of tests by various researchers. The nature of those tests has not been found, but it seems reasonable to suppose that the Eurocode method's omission of the foundation modulus is due to the difficulty in its measurement and calculation.

In contrast, Japanese design guidance [4], cited by Hwang and Komatsu [5], allows the stiffness of a connection to be calculated based on the empirically-derived foundation modulus for the timber surrounding the connector. The deformation of the connector and the geometry of the connection are then allowed for in a beam-on-elastic-foundation model.

The use of the foundation modulus in the stiffness calculation means that the geometry of the connection can be allowed for, in particular the length of the dowel and its consequent deformed shape. No analytical or numerical calculation method has so far been adopted for the foundation modulus. Its measurement by experiment is also difficult, since it is not possible to create a test in which the dowel passes through a hole in the timber and remains rigidly straight under load [6]. Measurements of the foundation modulus, therefore, need to be corrected for dowel deformation, and it may be this difficulty in predicting the foundation modulus which has led current design guidance to omit it from methods to predict stiffness, instead directly calculating the overall stiffness.

The main obstacle to the derivation of a model for the foundation modulus is the nonlinear behaviour observed under initial load. Even with a tight-fitting dowel, the connection stiffness is initially very low, and gradually rises as the load increases, going through a region of relatively constant stiffness until plastic behaviour begins to occur [7]. The unloading path has a much higher stiffness than the loading path, resulting in a residual displacement upon removal of the load. Dorn argues that this behaviour is a result of the contact behaviour between the face of the dowel and the timber, as the imperfections in the timber surface are crushed under the applied load.

2 Stress function model

It has been shown [8] that, after repeated cyclic loading, the embedment stiffness of a block of timber tended towards that predicted by elastic analysis. Using an analytical model for the elastic stiffness of a pin-loaded plate, with the geometry shown in Figure 1, equations can therefore be derived for the embedment stiffness of timber under cyclic load.

The mathematical form for such a model has been derived by several researchers [9-12] based on the underlying theory of orthotropic plates by Lekhnitskii [13], who showed that the general form of the stress functions for an infinite orthotropic plate with a hole is as given by (1) to (4). Finding the solution for a particular applied load relies on finding the coefficients a_n and b_n which correspond to the distribution of the load on the edge of the hole. ζ_n are transformed coordinates describing the point on the plate under consideration. The complex stress functions and ϕ_1 and ϕ_2 are defined so that the displacements u in the direction of the applied force are given by (5). i is the imaginary unit. These infinite-plate displacements u allow relative displacements to be calculated between points. This is done by superposition, as presented in Section 2.1.

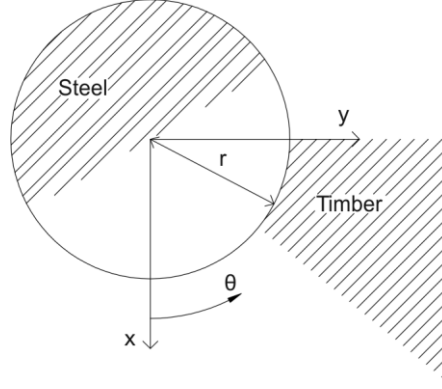


Figure 1 - Geometry and notation for stress function model

$$\Phi_1 = a_0 \ln \zeta_1 + \sum_{n=2}^{\infty} \frac{a_n}{\zeta_1^n} \quad (1)$$

$$\Phi_2 = b_0 \ln \zeta_2 + \sum_{n=2}^{\infty} \frac{b_n}{\zeta_2^n} \quad (2)$$

$$\zeta_1 = \frac{z_1 + \sqrt{z_1^2 - r^2(1 + \mu_1^2)}}{r(1 - i\mu_1)} \quad z_1 = x + \mu_1 y \quad (3)$$

$$\zeta_2 = \frac{z_2 + \sqrt{z_2^2 - r^2(1 + \mu_2^2)}}{r(1 - i\mu_2)} \quad z_2 = x + \mu_2 y \quad (4)$$

$$u = 2\text{Re}(p_1 \Phi_1 + p_2 \Phi_2) + U \quad (5)$$

$\text{Re}()$ denotes the real part of what is, in general, a complex number in the brackets. u is the displacement in the x direction relative to a particular fixed point, and so includes a constant of integration, U . μ_1 , μ_2 , p_1 , p_2 , q_1 and q_2 are derived from the material properties of the plate material, the timber, as in Equations (6) to (9), where E_1 is the elastic modulus of the plate material in the x direction, E_2 the elastic modulus in the y direction, G is the shear modulus, and ν_1 the Poisson's ratio.

$$\mu_1 = \sqrt{\frac{(2\nu_1 - \frac{E_1}{G}) + \sqrt{(2\nu_1 - \frac{E_1}{G})^2 - 4\frac{E_1}{E_2}}}{2}} \quad \mu_2 = \sqrt{\frac{(2\nu_1 - \frac{E_1}{G}) - \sqrt{(2\nu_1 - \frac{E_1}{G})^2 - 4\frac{E_1}{E_2}}}{2}} \quad (6)$$

$$p_1 = \frac{\mu_1^2}{E_1} - \frac{\nu_1}{E_1} \quad p_2 = \frac{\mu_2^2}{E_1} - \frac{\nu_1}{E_1} \quad (7)$$

$$q_1 = \frac{1}{\mu_1 E_2} - \frac{\nu_1 \mu_1}{E_1} \quad q_2 = \frac{1}{\mu_2 E_2} - \frac{\nu_1 \mu_2}{E_1} \quad (8)$$

$$a_0 = \frac{1}{\pi} \frac{i\mu_1(1 + (\nu_1 E_2/E_1)(i\mu_2)^2)}{2((i\mu_2)^2 - (i\mu_1)^2)} \quad b_0 = \frac{1}{\pi} \frac{i\mu_2(1 + (\nu_1 E_2/E_1)(i\mu_1)^2)}{2((i\mu_1)^2 - (i\mu_2)^2)} \quad (9)$$

The general solution by Lekhnitskii [13] is a stress function for an infinite orthotropic plate in plane stress, with a hole loaded on its edge. Hyer and Klang [11] applied the general complex Fourier series to the plate, and related the values of the coefficients a_n and b_n in (1) and (2) to the Fourier coefficients by equating the forces at the hole edge. The boundary conditions at the hole edge and the derivation of the coefficients are described in Hyer and Klang's paper. The same approach was used in this study.

2.1 Using the stress function to calculate displacements

The solution can then be translated and superimposed to estimate the relative displacements between dowels. This method is appropriate when the free edges of the timber do not significantly affect the distribution of stress, an approximation which is reasonable for calculation of the rotational stiffness of a moment connection, where all the timber subject to significant stress is between the dowels forming the couple. The superposition for two dowels forming a couple is shown in Figure 2, as well as configurations for two closely-spaced dowels transmitting a compressive force, and a dowel supported by a rigid foundation.

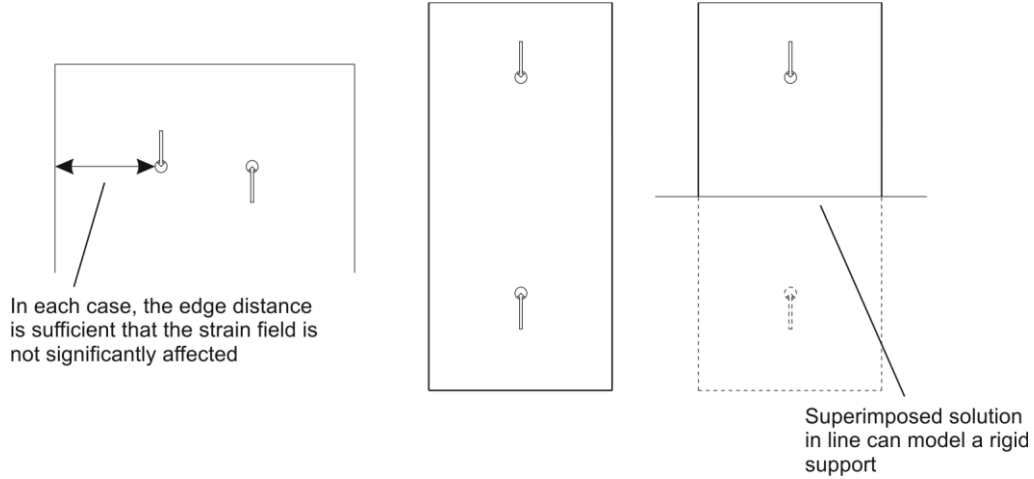


Figure 2 – Superimposing infinite-plate stress functions to model different orientations of connections

To allow for a non-zero far-field stress, Echavarría [12] added the stress function for a stretched plate to that for the pin-loaded plate. The general form of the stress function for a pin-loaded stretched plate, subject to a uniform tensile stress of $p/2$, is given by (10) and (11).

$$\phi_1 = Pa_0 \ln \zeta_1 + \frac{p}{2} \left(\frac{1}{\zeta_1} \left(\frac{-i}{\mu_1 - \mu_2} \right) + \frac{z_1}{\mu_1^2 - \mu_2^2} \right) + \sum_{n=1}^{\infty} \frac{a_n}{\zeta_1^n} \quad (10)$$

$$\phi_1 = Pb_0 \ln \zeta_2 + \frac{p}{2} \left(\frac{1}{\zeta_2} \left(\frac{-i}{\mu_2 - \mu_1} \right) + \frac{z_2}{\mu_2^2 - \mu_1^2} \right) + \sum_{n=1}^{\infty} \frac{b_n}{\zeta_2^n} \quad (11)$$

Each stress function in (10) and (11) can be broken down into three parts:

- the term in $\ln \zeta_{1,2}$ represents the net force applied to the hole edge, causing the movement of the hole, with unchanged size and shape, through the timber;
- the term in p represents the constant value towards which the stress in the member tends, far from the hole, stretching or compressing the plate; and
- the terms in $1/\zeta_{1,2}^n$ represent the change in shape of the hole itself, none of them applying a net force to the hole boundary, so that their effect is confined to the area immediately around the connector.

The three components are illustrated in Figure 2 for a single-dowel linear connection. The displacement field is formed by superimposing two infinite plate solutions, including the stretched-plate component, either side of the line of symmetry shown in the figure. The edge distances required in timber connections to prevent splitting ensure that edge effects do not significantly change the local stresses and strains around the hole described by the $1/\zeta_{1,2}^n$ terms, so they present a reasonable model of the deformed shape of the hole.

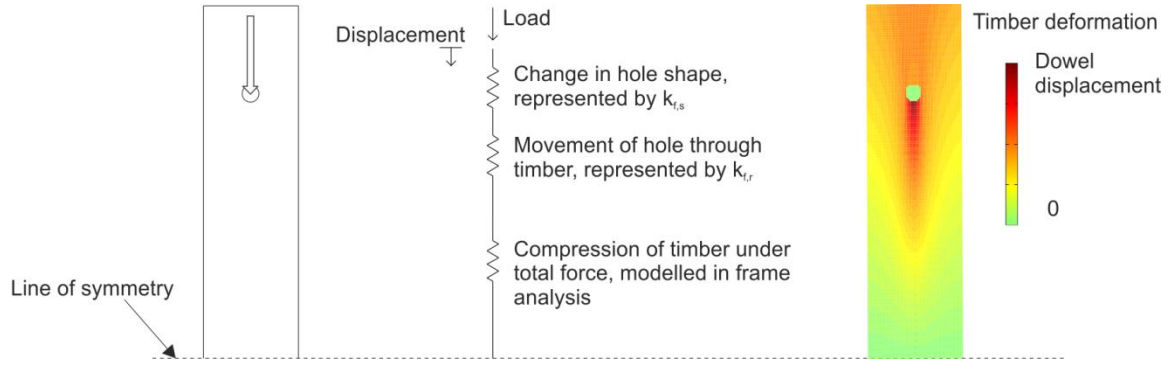


Figure 3 - Components of dowel movement in a linear connection, and the full displacement field given by the stress function

2.1.1 Simplification to form a design method

For simplification of the above equations into a method suitable for hand calculation, the division of the stress function solution into parts is convenient. The part of the stress function which represents the change in the shape of the hole is seen to dissipate quickly with distance from the hole: for the material properties of the Norway spruce used in these tests, loaded parallel-to-grain, it reduces to below 20% of its peak after 7 times the hole diameter in the loaded direction and 2 times the diameter perpendicular. The edge-distances and spacing required to prevent splitting therefore ensure that the edge of the timber and the presence of other dowel holes do not significantly effect this part of the stress function. As a result, it can be considered to be a property of the timber, in the same way as K_{ser} is in Eurocode 5. The calculation process can therefore be greatly simplified by tabulating this value for each timber grade.

The part of the stress function which represents the far-field stress is only necessary in cases where edge effects lead to the development of a constant stress in the distance between the dowels, such as in the translational movement of a connection to a beam or column. In that case, the effect of this constant stress is simply to produce a constant strain in the member, and this is considered in a normal frame analysis, independently of the connections. In calculating the semi-rigid connection stiffness for frame analysis, therefore, this component of deformation can be omitted.

If the component relating to the change in hole shape is tabulated, and the far-field stress omitted, then only one term remains in the equation for the stress function. It represents the movement of the circular hole relative to the timber around it, the 'rigid insert' displacement. The stress functions Φ_1 and Φ_2 for this term are given in (11), and is then used to find the displacement in the x-direction by (12) to (14), which can be simplified to (15). l is the distance between the connections as a multiple of the hole diameter.

$$\Phi_1 = a_0 \ln \zeta_1 \quad \Phi_2 = b_0 \ln \zeta_2 \quad (11)$$

$$u_0 - u_l = -2P(p_1 a_0 \ln \frac{\zeta_{1,0}}{\zeta_{1,l}} + p_2 b_0 \ln \frac{\zeta_{2,0}}{\zeta_{2,l}}) \quad (12)$$

$$\frac{\zeta_{1,0}}{\zeta_{1,l}} = \frac{1+i\mu_1}{2l+\sqrt{4l^2-1+(i\mu_1)^2}} \quad (13)$$

$$\frac{\zeta_{2,0}}{\zeta_{2,l}} = \frac{1+i\mu_2}{2l+\sqrt{4l^2-1+(i\mu_2)^2}} \quad (14)$$

$$u_0 - u_l = -2P(p_1 a_0 \ln \frac{1+i\mu_1}{4l} + p_2 b_0 \ln \frac{1+i\mu_2}{4l}) \quad (15)$$

Since μ_1 and μ_2 are purely imaginary quantities, $p_1 a_0$, $p_2 b_0$, $i\mu_1$ and $i\mu_2$ are four real-valued material properties which describe the orthotropic elastic behaviour of the timber,

and can be calculated from the four independent elastic properties of the timber: the two elastic moduli, the shear modulus and the Poisson's ratio. Relabeling $p_1 a_0 = \beta_1$, $p_2 b_0 = \beta_2$, $i\mu_1 = \alpha_1$ and $i\mu_2 = \alpha_2$, the four properties are given by (16) and (17).

$$\alpha_1 = \sqrt{\frac{\frac{E_1}{G} - 2\nu_1 + \sqrt{(2\nu_1 - \frac{E_1}{G})^2 - 4\frac{E_1}{E_2}}}{2}} \quad \alpha_2 = \sqrt{\frac{\frac{E_1}{G} - 2\nu_1 - \sqrt{(2\nu_1 - \frac{E_1}{G})^2 - 4\frac{E_1}{E_2}}}{2}} \quad (16)$$

$$\beta_1 = \frac{1}{\pi} \frac{\alpha_1(1 + (\nu_1 E_2 / E_1)(\alpha_2)^2)}{2((\alpha_1)^2 - (\alpha_2)^2)} \left(\frac{\alpha_1^2}{E_1} + \frac{\nu_1}{E_1} \right) \quad \beta_2 = \frac{1}{\pi} \frac{\alpha_2(1 + (\nu_1 E_2 / E_1)(\alpha_1)^2)}{2((\alpha_2)^2 - (\alpha_1)^2)} \left(\frac{\alpha_2^2}{E_1} + \frac{\nu_1}{E_1} \right) \quad (17)$$

The rigid insert stiffness for a linear connection can then be represented as $k_{f,r}$ in (18), where l represents the linear distance between connections, i.e. the length of the member.

$$k_{f,r} = \frac{1}{2(\beta_1 \ln \frac{1+\alpha_1}{4l} + \beta_2 \ln \frac{1+\alpha_2}{4l})} \quad (18)$$

For a moment connection, the rigid insert stiffness can be obtained by a similar method, and is given by (19), where l is now the distance between the connector and the centroid of the connection as a multiple of the hole diameter.

$$k_{f,r} = \frac{1}{2(\beta_1 \ln \frac{1+\alpha_1}{2l\alpha_1} + \beta_2 \ln \frac{1+\alpha_2}{2l\alpha_2})} \quad (19)$$

The foundation modulus can then be calculated by combining the stiffness associated with the change in hole shape $k_{f,s}$, which could be derived from (10) and (11) and tabulated for a particular timber grade, with the rigid insert stiffness $k_{f,r}$, which depends on the geometry of the structure and connection, using (20). For the Norway spruce used in these tests, $k_{f,s}$ is 3536N/mm/mm parallel and 857N/mm/mm perpendicular to grain.

$$k_f = \left(\frac{1}{k_{f,r}} + \frac{1}{k_{f,s}} \right)^{-1} \quad (20)$$

2.1.2 Beam on Elastic Foundation

The complex stress function model gives an estimate of the stiffness of the timber in embedment in each plane along the length of the dowel. This stiffness can then be used as the foundation modulus for a beam-on-elastic-foundation model of the complete dowel. The geometry of the dowel in both a connection with a central flitch plate, for example, could be simplified to be represented as a beam on elastic foundation with a central point load.

The deflection under a point load of an infinitely long circular beam on elastic foundation, at the point where the load is applied, is given by (21), where k_f is the foundation modulus determined from the embedment behaviour of the timber, d is the diameter of the connector and E_s is the elastic modulus of the connector material.

$$K_{dyn} = d(\pi k_f^3 E_s)^{\frac{1}{4}} \quad (21)$$

2.1.3 Design Method

The design method for a single connector can therefore be summarized as:

- read tabulated values of $k_{f,s}$ for standard timber grades,
- calculate $k_{f,r}$ using (16), (17), (18) and (19) for the geometry in question,
- calculate the foundation modulus according to (20) and
- calculate the stiffness for a single connector according to (21).

The stiffness K_{dyn} can then be used along with conventional design methods to assess the translational and rotational stiffness of connections.

3 Verification by Physical Tests

The method was verified using test results from simple structures made from glulam connected by dowel-type connections: a linear connection, a moment connection, and a complete portal frame. Each connection is formed by a central steel flitch plate and plain steel dowels. The stiffness of each could be identified either by making it part of a structure with imposed mass and using modal analysis techniques to identify its natural frequencies, or by applying an equivalent cyclic force and measuring displacement.

For the test of the moment connection and the frame, a modal test was possible. A mass was placed on a cantilever supported by a two-dowel moment connection, to give a static load of 20% of the predicted yield moment, which was considered representative of a connection in normal service. For the linear stiffness test, a servo-hydraulic loading machine was used to apply an equivalent cyclic load, and the displacement measured using a $\pm 1\text{mm}$ linear variable differential transformer. The specimens are shown in Figure 4.

In order to predict the stiffness of each connection, and therefore the natural frequency of the cantilever or frame, the principal elastic moduli were measured according to EN 408:2010 [14].

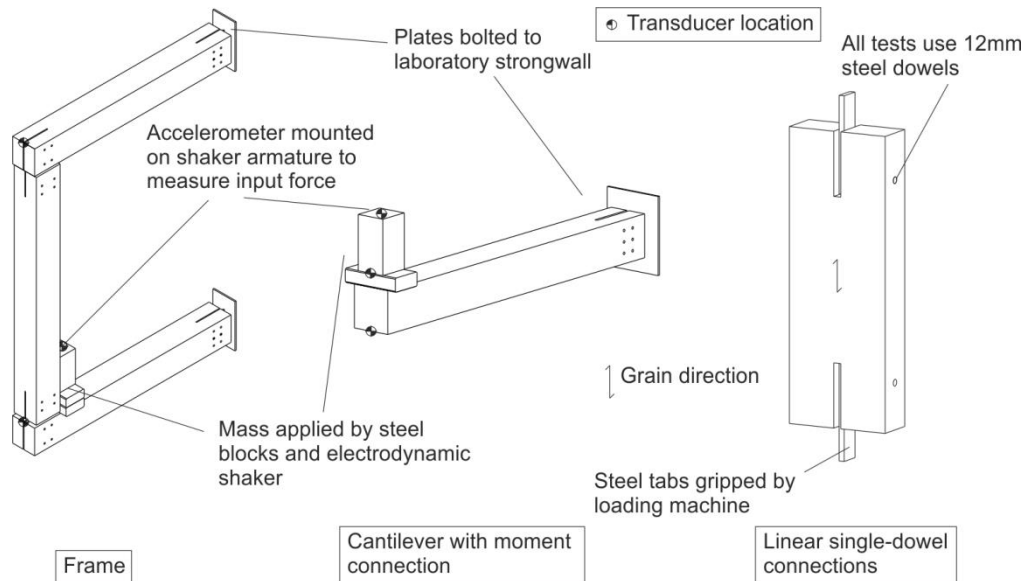


Figure 4 - Schematic test setup for tests on moment connections and frames

3.1 Results

3.1.1 Linear connection

The measured stiffness of the linear connection and its predicted stiffness based on the measured elastic moduli are shown in Figure 5. The results show a slight trend of increasing stiffness with the magnitude of the peak applied force. This is thought to be due to further compression of the contact surface between dowel and timber under higher loads, leading to a stiffness closer to that for a rigid contact surface.

The predicted stiffness was based on the mean elastic properties of specimens cut from the dynamic test pieces after testing. It represents a reasonable estimate of the stiffness under cyclic load. Under compressive load, the results at the higher peak applied force are

slightly higher than the predicted value. This is thought to be due to the inaccuracies inherent in this simplified approach, particularly the assumption of a Winkler foundation.

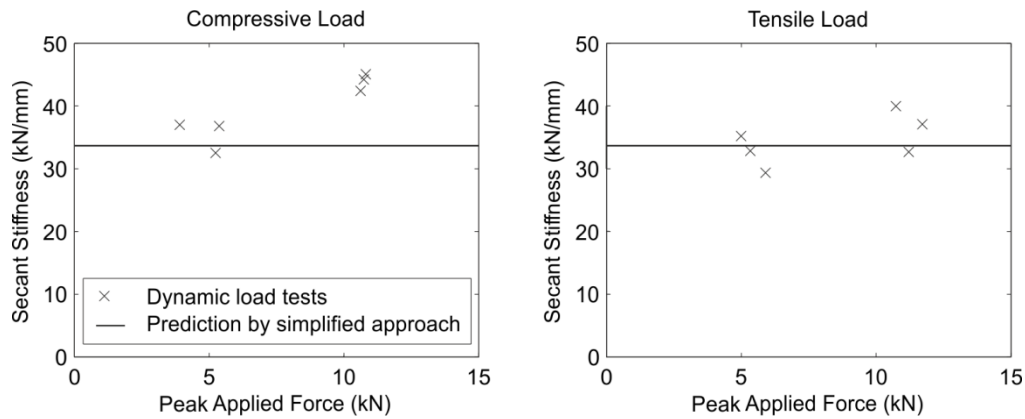


Figure 5 - Comparison of the results of the dynamic load tests on linear connections with the stiffness predictions by the simplified method

3.1.2 Moment connection

The linear connections tested were all single-dowel connections. A moment connection must have multiple dowels, but in its simplest form has just two. Figure 4 schematically shows the test setup used to test two- and six-dowel connections using an electrodynamic shaker.

Table 1 compares the measured natural frequencies with those predicted using the stress function model. It can be seen that, in the case of the two-dowel connection, the stress function model predicts the natural frequency with reasonable accuracy. In the six-dowel connection, the measured natural frequency is higher than the predicted value. It is thought that this is due to friction between the steel plate and the timber slot, since the steel plate was forced against one side of the slot by the installation of the dowels.

Table 1 - Test results for moment connections – measured frequency is the mean of two connections for the two-dowel tests and the result from a single connection for the six-dowel test

Number of dowels	Imposed mass	Predicted natural frequency	Measured natural frequency
2	37kg	8.86Hz	8.70Hz
6	67kg	7.67Hz	8.55Hz

3.1.3 Frame

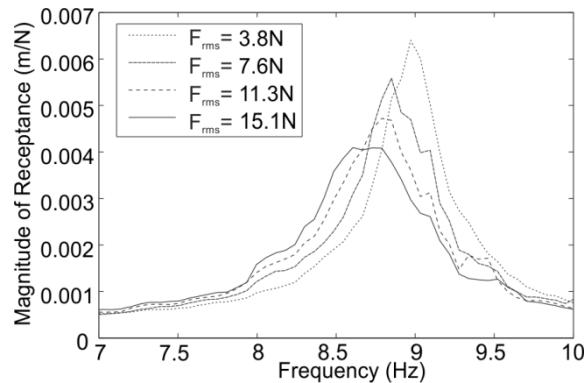
In the frame tests, the natural frequency was measured using both a pseudo-random cyclic load from an electrodynamic shaker and an impulse from an instrumented hammer. The amplitude of the movement induced by the shaker at resonance was higher than that caused by the hammer: the root mean square value of acceleration due to the shaker was approximately 0.40g, while the peak acceleration caused by the impulse from the hammer had a mean value of 0.38g over the tests. The nonlinearity in the connection stiffness meant that these two excitations resulted in different resonant frequencies.

The impulse was applied at the shaker location, with the shaker in position to ensure that the mass distribution was the same with each form of excitation. The natural frequencies obtained from the impulse tests are shown in Table 2.

Table 2 - Test results for frames

Frame	Measured natural frequency (Impulse hammer)	Predicted natural frequency
Frame A	9.13Hz	10.6Hz
Frame B	9.88Hz	10.6Hz

Using the electrodynamic shaker, the amplitude of the applied force could be varied. The variation of the natural frequency with amplitude is shown in Figure 6, which shows how the receptance function changes as the root mean square value of the force applied by the shaker is increased. The peak value of the receptance, which approximately corresponds to the natural frequency, moves to a lower frequency for higher amplitude of applied force. It is notable, however, that the peak magnitude of receptance also decreases with amplitude of load, since the increase in damping outweighs the greater flexibility of the system. A design case using the stiffness and damping at the lower amplitude is therefore likely to be the most onerous case.

**Figure 6 - Frequency response function for Frame A showing its variation with the magnitude of the applied force**

Using the stress function model, the rotational and translational stiffness of each of the connections in the frame was predicted. A stiffness matrix model, incorporating the bending and shear deformation of the beams as well as the predicted connection stiffness, was then constructed to assess the dynamic properties of the frame. The eigenvalues of the stiffness matrix gave estimates of the natural frequency, which are shown in Table 2. It is thought that the measured natural frequency is slightly lower than the predicted natural frequency because of the low mean load on some of the connections in the frame. While the connections at the wall were loaded to approximately 20% of their predicted failure load, the connections between members were only loaded to around 10%. The single-dowel connection tests showed that a lower mean force, equivalent to a lower peak applied force in Figure 5, resulted in a lower stiffness, and this was considered to be due to the contact surface between dowel and timber not having reached its full stiffness at low loads. As a brief comparison, using the Eurocode 5 method would predict a natural frequency a little over 6Hz for this frame.

4 Conclusion

The methods for prediction of connection stiffness in current design codes are empirically based. This method allows stiffness calculation based on material properties, and can be

applied, amongst other circumstances, to in-service vibration, such as that caused by footfall or turbulent wind load.

Previous work by the authors has shown that the embedment stiffness of a dowel in timber under the cyclic loads imposed by in-service vibration can be predicted using an elastic stress-function model, which can be expressed as a series of analytical equations. In this study, the model has been simplified into a set of equations amenable to calculation without specialist software, which have been tested for linear and moment connections in simple structures. The model has been shown to predict stiffness and natural frequency accurately in linear and moment connections. The experimental work presented here used small sample sizes, and a more thorough experimental validation will be required to prove the validity of the method in other configurations.

One of the potential advantages of this beam-on-foundation approach to connection stiffness is the ability to allow for the effect of the embedded length of the dowel. The simplified method presented here is just an approximation for a long dowel, but could be developed to allow for dowel length.

References

- [1] BS EN 1995-1-1:2004+A1:2008, *Eurocode 5 Design of timber structures Part 1-1: General — Common rules and rules for buildings*, BSI, 2009.
- [2] Porteous, J. & Kermani, A.: *Structural Timber Design to Eurocode 5*. Blackwell Oxford, 2007.
- [3] Ehlbeck, J. & Larsen, H. J.: Eurocode 5-Design of timber structures: Joints. In: *International workshop on wood connectors*, Madison, USA. Forest Products Society, 9-23, 1991.
- [4] *Wood structure design note (in Japanese)* Architectural Institute of Japan, 1995.
- [5] Hwang, K. & Komatsu, K. Bearing properties of engineered wood products I: effects of dowel diameter and loading direction. *Journal of Wood Science*, 48(4): 295-301, 2002.
- [6] Foschi, R. O., Yao, F. & Rogerson, D.: Determining Embedment Response Parameters from Connector Tests. In: *World Conference on Timber engineering*, Whistler, B.C., Canada. 2000.
- [7] Dorn, M., De Borst, K. & Eberhardsteiner, J. Experiments on dowel-type timber connections. *Engineering Structures*, 47(0): 67-80, 2013.
- [8] Reynolds, T. P. S., Harris, R. & Chang, W.-S. An analytical model for embedment stiffness of a dowel in timber under cyclic load. *European Journal of Wood and Wood Products*, 2013, 10.1007/s00107-013-0716-1.
- [9] De Jong, T. Stresses around pin-loaded holes in elastically orthotropic or isotropic plates. *Journal of composite materials*, 11(3): 313, 1977.
- [10] Zhang, K.-D. & Ueng, C. E. S. Stresses Around a Pin-loaded Hole in Orthotropic Plates. *Journal of composite materials*, 18(5): 432-446, 1984.
- [11] Hyer, M. & Klang, E. Contact stresses in pin-loaded orthotropic plates. *International Journal of Solids and Structures*, 21(9): 957-975, 1985.
- [12] Echavarría, C., Haller, P. & Salenikovitch, A. Analytical study of a pin-loaded hole in elastic orthotropic plates. *Composite Structures*, 79(1): 107-112, 2007.
- [13] Lekhnitskii, S. G.: *Anisotropic Plates*. Gordon and Breach New York, 1968.
- [14] BS EN 408:2010, *Timber structures. Structural timber and glued laminated timber. Determination of some physical and mechanical properties* BSI, 2011.